

Structuring Mobility Transition with An Adaptive Graph Representation

Tianlong Gu, Minfeng Zhu, Wei Chen, Zhaosong Huang, Ross Maciejewski, Liang Chang

Abstract—Modeling human mobility is a critical task in fields such as urban planning, ecology, and epidemiology. Given the current use of mobile phones, there is an abundance of data that can be used to create models of high reliability. Existing techniques can reveal the macro-patterns of crowd movement or analyze the trajectory of a person; however, they typically focus on geographical characteristics. This paper presents a graph-based approach for structuring crowd mobility transition over multiple granularities in the context of social behavior. The key to our approach is an adaptive data representation, the adaptive mobility transition graph, that is globally generated from citywide human mobility data by defining the temporal trends of human mobility and the interleaved transitions between different mobility patterns. We describe the design, creation and manipulation of the adaptive mobility transition graph and introduce a visual analysis system that supports the multi-faceted exploration of citywide human mobility patterns.

Index Terms—Timeline, Mobility, Mobility Transition, Mobility Patterns

I. INTRODUCTION

THE rapid deployment of location-aware devices has made it easy to collect large amounts of trajectory data from humans. The abundance of such data is providing new insights across a variety of application domains including urban planning, transportation management, and epidemiology [10], [12], [22]. In such domains, developing insights into human mobility patterns [4] can enable researchers to develop models of disease spread, traffic patterns, etc., where analysts explore mobility patterns [34] to identify potential drivers and their consequences. Given the abundance of trajectory data, a variety of modeling, analysis and visualization tools have been developed to explore mobility patterns. Recent work (e.g., [41], [39]) has focused on developing rules of human mobility by semantically linking trajectory data to physical points-of-interest. Previous solutions emphasize visualization for mobility patterns. The mobility pattern is defined as a group of trajectories which imply similar behaviors (e.g., staying at home, driving). However, little attention has been given to the transition between mobility patterns. For instance,

a person stops visiting and takes a meal at the restaurant. We are interested in analyzing the time and location of the transition between visiting and eating. One pioneering work [35] employed a Dynamic Categorical Data View to visualize state transitions over time. However, this approach only shows the transition between different locations as opposed to summarizing overall patterns and trends. As such, new work is needed to extract and summarize generalizable mobility patterns. This requires novel methods for both data aggregation that can match an analyst’s mental model of spatiotemporal trends (rush hour times versus mid-day traffic or city-center versus rural commutes) and for visual representations that can effectively summarize large amounts of trajectories into a manageable exploratory view.

We propose a novel representation, the adaptive mobility transition graph (AMTG), to model the temporal evolution of human mobility patterns of massive crowds. An AMTG contains not only nodes representing mobility patterns but also edges representing transitions between crowd behavior. Our proposed methodology focuses on enabling a flexible/adaptive partitioning of the data. Where many techniques for trajectory analysis simply uniformly partition trajectories over time, we propose segmenting the data in a semantically meaningful way to better capture human behaviors. The computation of an AMTG consists of three major stages. First, a trajectory is partitioned into a series of episodes (stop and move) adaptively according to human behaviours. Second, the mobility pattern is constructed by encoding the mobility of a trajectory segment with feature descriptors and clustering similar segments. Third, the probability of mobility transitions is estimated by means of a time-varying dynamic Bayesian network [32].

To support effective analysis of a constructed AMTG, we have designed and implemented an interactive visual analysis system that enables a multi-faceted exploration of the spatiotemporal evolutions and transitions between mobility patterns. The visual interface employs a parallel coordinates view and geographical map view to help users comprehend and compare the difference between patterns. The main view for the adaptive mobility transition graph shows a high level of transitions between mobility patterns. With our system, users are able to quickly browse the summarized information and investigate human mobility at both the crowd scale and the person scale, thereby tracing the dynamic evolution of human mobility patterns. Our contributions include:

- A new scheme that represents and constructs mobility patterns from raw trajectory data;
- A visual analysis system that supports the exploration of citywide human mobility patterns.

T.Gu and L.Chang are with Guangxi Key Lab of trusted software, Guilin University of Electronic Technology. E-mail: cctlgu@guet.edu.cn; changl@guet.edu.cn

W.Chen is with The State Key Lab of CAD & CG, Zhejiang University and also with the Joint Institute of Frontier Technologies, Alibaba-Zhejiang University. E-mail: chenwei@cad.zju.edu.cn

M.Zhu and Z. Huang are with State Key Lab of CAD&CG, Zhejiang University. E-mail: minfeng_zhu@zju.edu.cn, zshuang02@gmail.com

R.Maciejewski is with School of Computing, Informatics & Decision Systems Engineering, Arizona State University. E-mail: rmacieje@asu.edu

T.Gu and M.Zhu contributed equally to this work and share first authorship. L.Chang is the corresponding author.

II. RELATED WORK

A. Mobility Models

Mobility models aim to simulate human movement behavior in urban areas, and such models play an important role in mobile network construction and new communication technology development [34]. Many models assume that the movement is random. In the Random Walk Mobility Model [7], a person starts from a position at a given point and moves at a random distance and angle towards a destination. In the Random Waypoint Mobility Model [27], persons move from location to location with random stops in between. In the Smooth Mobility Model, an accelerated velocity is employed to eliminate sharp trajectory turns and sudden changes of speed [6], and in the Reference Point Group Mobility Model [37], the mobility of a simulated trajectory can be randomly influenced by other neighboring nodes. Given that such randomness often results in unrealistic patterns, other models have been developed to try and link features of the built environment to the mobility patterns. For example, the Scalable Mobility Model [5] adopts three sub-models, a physical model, a gravity model and a fluid model, to characterise population distribution, mobility classes and transition probability. Other works focus on using a transition matrix to reflect the probability of moving to an adjacent cell [8], and the Mask Based Mobility Model [16] divides the simulated environment into square cells where the probability of moving from one cell to another is modeled by integrating geographical, topographical and economic data.

B. Mobility Analysis

Lu et al. [22] studied the movement of 1.9 million mobile phone users during an earthquake and found that the predictability of population movements during a disaster was higher than previously thought, and Gonzalez's work confirmed that up to 90% of the different mobility networks could be described using only 17 different motifs [11]. Wang et al. [38] used individual road segments to trace driver sources which enables the development of a bipartite network framework of road usage. Furthermore, a method to cluster road usage for improving road network efficiency has also been proposed [36]. Recently, semantic trajectory analysis has also attracted much attention. Spaccapietra et al. [33] proposed to transform a trajectory into move and stop segments. In order to enrich semantic, Yan et al. [40] introduced a semantic model to integrate stops and moves with geographic knowledge. More recent work has proposed the semantic analysis of trajectories for locating billboards [20], transforming trajectories into documents to support text searches [1], and using topological methods to capture spatiotemporal variations within a city [25].

C. Trajectory Clustering

Clustering analysis is one of the general approaches to studying large datasets since it allows the analyst to focus on a higher level representation of the data [2]. Methods for clustering trajectories aim to group similar trajectories having similar attributes. As Kisilevich et al. [18] gave a survey about

clustering methods on trajectory data, we briefly review the most relevant methods here.

Density-based methods use a threshold for each object to overcome issues with noisy data [30]. The OPTICS method [3] created a cluster-ordering which represents its density-based clustering structure. Lee et al. [19] proposed the TRACLUS algorithm. This method first partitions a trajectory into segments and then groups similar segments into a cluster. Distance-based clustering methods first transform trajectories into feature vectors. Each feature represents single characteristic of the original object (e.g., direction). Then feature vectors are grouped using generic clustering algorithms (e.g., K-means). Sometimes, distance functions are defined on features, such as direction or speed, for classifying trajectories [28].

D. Visualization of Mobility Transitions

One common means of exploring mobility data is through visualization, and a large body of visualization research has focused on the evolution of patterns and flow of spatiotemporal information. For example, stacked graph representation schemes [15] and Sankey diagrams [29] have been widely used to describe the evolution of categorical data over time. However, these techniques tend to ignore how information evolves and transitions. While many visualization methods have focused on the flow of text, other recent work has focused on urban computing and spatiotemporal distribution characteristics of trajectories. VATT [9] and MovementSlicer [14] employed a storyline-based approach to visualize the evolution of each person. However, these approaches only support a small number of persons. Landesberger et al. [35] designed the Dynamic Categorical Data View to support the visual exploration of categorical (e.g., location) changes of large numbers of persons. However, this work consider the changes between two time points. They ignore the changes along two consecutive time points. Our approach focuses on constructing mobility patterns from trajectory data and visually analyzing continuous transitions over time.

TABLE I
MATHEMATICAL NOTATIONS

Symbol	Description
\mathbf{R}	A raw trajectory
\mathbf{r}_i	Trajectory points
\mathbf{R}_{seg_i}	The i -th segment of trajectory \mathbf{R}
τ	Time threshold
δ	Distance threshold
\mathbf{F}_i	The feature vector of trajectory segment \mathbf{R}_{seg_i}
\mathbf{MP}	The set of mobility patterns
\mathbf{m}_i	The mobility vectors of trajectory segment \mathbf{R}_{seg_i}
$\mathbf{G} = (\mathbf{V}, \mathbf{E})$	A directed graph representation of AMTG
$V_j^{t_i}$	A node of mobility pattern \mathbf{MP}_j at t_i
\mathcal{V}^{t_i}	A set of nodes at t_i
\mathbf{A}^{t_i}	A transition matrix \mathbf{A}^{t_i} between \mathcal{V}^{t_i} and $\mathcal{V}^{t_{i+1}}$
\mathbf{M}	Trajectory data
m_i^l	The mobility vector of the i -th segment of person l
\mathbf{T}	Time points of trajectory segments
t_i^l	The end time of the i -th segment of person l

III. METHOD

In order to better understand spatiotemporal data, we need to extract *stops* and *moves* which imply human behaviors.

Stops are the places people stay for long periods, while *moves* are routes between different places. It is valuable to study the transition between human behaviors to discover patterns and gain insight into human mobility. Analyzing how people transfer between different behaviors or locations gives us an overview of the lifestyle of a city.

The mobile trajectory data employed in our study is provided by a mobile phone service company. Our dataset includes 14 billion records of 7 million mobile users during the period from January, 2014 to February, 2014. Each record contains multiple items: a phone ID, a cell tower ID, and a time stamp. In this section, we introduce our method to extract mobility patterns and generate their transitions from trajectory data. For clarity, Table I lists the notations used in this paper.

A. Task Analysis and Design Rationale

Our goal is to characterize human mobility with the assistance of the construction and exploration of transitions among time-varying human mobility. We aim to summarize mobility patterns and explore regions with different mobility patterns. To address the problem, here are the analytical tasks that our visual analytics interface should support:

- T1** *Explore the overall mobility transition:* The new representation should provide an overview of sequential transitions among various mobility patterns. To understand human movement behavior, interesting transitions need to be identified and explored.
- T2** *Explore and evaluate the feature descriptors:* We need to analyze the distribution and examine the effectiveness of the attributes of trajectories.
- T3** *Study the specific mobility patterns:* There is a need to enable investigations of mobility patterns and track dynamic transitions across different mobility patterns.
- T4** *Query trajectory of specific persons:* In addition to the macroscopic description of crowd mobility, it is desirable to search persons by their mobility behavior.

To handle **T1**, the system should provide the overview of a set of mobility patterns and their transition relationships. The analysts are interested in transitions that occur with a high probability and want to explore detailed information about these transitions through visual interaction. We group similar trajectory segments from different persons into mobility patterns and generate a transition graph to characterize transitions.

For **T2**, our goal is to present the distribution of the feature descriptors extracted from trajectory segments. For high dimensional data, a scatter plot focuses on revealing the correlations between dimensions. Dimensionality reduction techniques generate embeddings in a low-dimensional space where the axes is not directly correspond to the original dimensions [21]. Hence, we employ the parallel coordinates plot to show the distribution of each feature descriptor.

For **T3**, it is necessary for analysts to explore the mobility patterns related to specific transitions. Our system allows the users to click-and-select a mobility pattern. The selected mobility pattern and the related transitions will be highlighted, and the analysts can trace the mobility transition over time.

To support **T4**, we design three query conditions, including ID, residence locations, and mobility patterns. The trajectories

of selected persons will be shown on the map. Analysts can query and compare the trajectory of persons in different regions or with specific behaviors.

B. Overview

Our approach consists of three stages: trajectory segmentation, mobility pattern construction, and AMTG generation.

Trajectory segmentation: We extract trajectory segments from a trajectory: a *stop* is an interesting place where a moving person stopped for a long period of time for an activity, such as sleeping, working or shopping. We partition a trajectory into a series of episodes by detecting stop segments.

Mobility pattern construction: For trajectories of a city-wide population, it is inefficient to study human mobility individually. Instead, it is more desirable to encode the segments with feature descriptors and group similar trajectory segments from different persons into mobility patterns.

AMTG generation: In this stage, we generate the adaptive mobility transition graph to characterize the temporal evolutions and interleaved transitions of mobility patterns. The AMTG takes a directed graph representation where nodes represent mobility patterns, and a directed edge indicates the transfer processes between pairs of nodes.

C. Adaptive Trajectory Segmentation

We describe a methodology to detect the stay location from a trajectory adaptively according to human behaviors. This segmentation approach is the adaptive portion of the AMTG.

1) *Trajectory Data:* Our method starts with raw trajectory records of a moving person. Such data is typically represented as a sequence of spatiotemporal records $\mathbf{r} = (x, y, t)$, yielding:

$$\mathbf{R} = \{\mathbf{r}_1, \mathbf{r}_2, \dots, \mathbf{r}_l\} \quad (1)$$

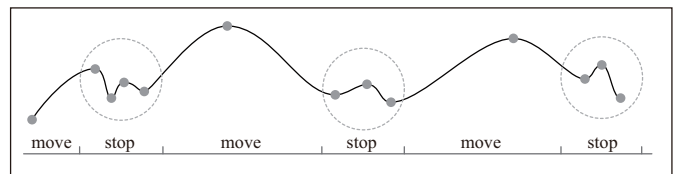


Fig. 1. The trajectory is divided into multiple segments by identifying stop records. Each grey dot indicates a record of the trajectory. The dotted circles represent detected stop trajectory segments.

2) *Trajectory Segmentation:* To characterize the mobility of a person, the sequence of location records needs to be classified into intervals that explicitly reflect various behaviors as shown in Figure 1. The first step is transforming raw trajectories into *stops* and *moves*, which can be used to detect places, such as residences and offices, where people stay for long periods. Density-based methods [42] use the fact that trajectory records of *stops* must be close to stay regions and stays should occur for a long period of time. A raw trajectory \mathbf{R} can be denoted as:

$$\mathbf{R} = \{\mathbf{R}_{seg_1}, \mathbf{R}_{seg_2}, \dots, \mathbf{R}_{seg_n}\} \quad (2)$$

$$\mathbf{R}_{seg_i} = \{\mathbf{r}_{i_1}, \mathbf{r}_{i_2}, \dots, \mathbf{r}_{i_n}\}, i = 1, \dots, n \quad (3)$$

where $\mathbf{r}_{i_j} = (x_{i_j}, y_{i_j}, t_{i_j})$, $1 \leq i_j \leq i_n$. \mathbf{R}_{seg_i} is considered as a *stop* trajectory segment when it meets three conditions [42] given a time threshold τ and a distance threshold δ :

- C1: the time difference between its first and other records should be larger than τ :

$$\|t_{i_1} - t_{i_n}\| \geq \tau$$

- C2: the location difference between its first and other records should be less than δ :

$$\forall 1 \leq j \leq i_n, \|(x_{i_1} - x_j, y_{i_1} - y_j)\|_2 \leq \delta$$

- C3: \mathbf{R}_{seg_i} is a maximum subsequence in \mathbf{R} :

$$\|(x_{i_1} - x_{i_{+1}}, y_{i_1} - y_{i_{+1}})\|_2 \geq \delta$$

Our method starts with the first unlabeled record. We constantly expand the segment by adding the next record if C2 is met. The segment expansion is stopped when C3 will be not fulfilled. If the segment also meet C1, we label all records of this segment as stop records. If not, we label the first unlabeled record as a move record. This process is repeated until all records have been assigned with a label. We can segment the trajectory according to their label. We refer each trajectory segment to *move* or *stop* with two time stamps, t_{start} and t_{end} , yielding a sequence of *move* or *stop* trajectories.

3) *Parameter Selection*: Selecting an appropriate value of τ and δ is not easy. A high time threshold will lead to the discovery of places where a person stayed for a long period of time, such as home or work. However, a small value for the time threshold allows analysts to identify more places where a person stayed for a few minutes, such as a bus stop or train station. In our dataset, the average time duration between two consecutive records is 68 minutes. 76.16% of the time duration is less than 30 minutes. Hence, we consider 60 minutes to be a suitable time threshold.

Stay behaviour may occur in two cases. If a person remains stationary for a time period, the positions keep being recorded when this person stays at office or home. In other cases, people walk around within a certain spatial region, for example, when people exercise or go to the park or market. The average distance between base stations is 0.539km, with 86.96% of the base station distance being less than 1km apart. The average distances between two consecutive records is 0.881km, and 75.17% of the recorded distances are less than 1km. Thus, we set δ to 1000 meters to detect stop records. In our experiments, if a person spent more than 60 minutes where all location references are within a distance of 1000 meters from each other, the trajectory segment is defined as a *stop*.

D. Mobility Pattern Construction

We describe how to construct mobility patterns by clustering trajectory segments based on extracted relevant feature vectors.

1) *Mobility Features*: To capture features of human mobility previous solutions typically cluster trajectories that share similar characteristics such as speed and direction or solutions that attempt to identify a group of persons who move together [24]. We focus on choosing features which describe the behavior of trajectories and are able to

separate different mobility patterns. We consider two kinds of feature descriptors: entropy for time series data and well-established geographic information. Entropy is one of the most fundamental quantities for describing the degree of predictability when characterizing a time series [26]. We adopt entropy as proposed in [31], which shows a 93% potential predictability in human mobility, and extend this work to temporal-correlations. The radius of gyration interprets the distance travelled by a user [12] which is used to separate mobile phone users into several groups. In order to capture the transition of different mobility patterns in different places, we use geographic centroids to describe the location of trajectory segments. For example, it is possible that a person who lives in suburban areas goes to work downtown by the subway. Thus, we also compute geographic features, such as the radius of gyration, centroid location, speed, etc. Then we can analyze the movement of the workplace and sightseeing of the city. We compute 8 feature descriptors that form a vector \mathbf{F}_i from a given trajectory segment \mathbf{R}_{seg_i} :

- **Temporal-uncorrelated Entropy** Song et al. [31] proposed a set of entropy-based measures to model human mobility. The temporal-uncorrelated entropy describes the probability of being observed at different places. We adopt the temporal-uncorrelated entropy because of its capability of distinguishing different movements:

$$S^{unc} = - \sum_{k=1}^N P(k) \log_2 P(k), P(k) \propto \sum_{j=i_1}^{i_n} I_k(\mathbf{r}_j)$$

where N is the number of places visited and $P(k)$ denotes the probability of a person visiting place k , $P(k) = \sum_{j=i_1}^{i_n} I_k(\mathbf{r}_j) / \sum_k \sum_{j=i_1}^{i_n} I_k(\mathbf{r}_j)$. I_k is an indicator function, where $I_k(\mathbf{r}_j) = 1$, if \mathbf{r}_j belongs to place k , else $I_k(\mathbf{r}_j) = 0$.

- **Temporal-correlated Entropy** We extend S^{unc} to the case of temporal correlation. A person is more likely to return to place k if the person stayed for a long time.

$$S^{tc} = - \sum_{k=1}^N P(k) \log_2 P(k)$$

$$P(k) \propto \sum_{j=i_1}^{i_n} I_k(\mathbf{r}_{i_j}) (t_{j+1} - t_{j-1}) / 2$$

- **Centroid Location** is the geographic centroid (the longitude and the latitude) of the trajectory segment:

$$\mathbf{CL} = \frac{1}{i_n - i_1 + 1} \sum_{j=i_1}^{i_n} \mathbf{r}_j$$

- **Radius of Gyration** describes the range in which a person tends to move around [12]. The radius of gyration is defined as:

$$r_g = \sqrt{\frac{1}{i_n - i_1 + 1} \sum_{j=i_1}^{i_n} \|\mathbf{r}_j - \mathbf{CL}\|_2^2}$$

where \mathbf{CL} is the centroid location defined above.

- **Residence Location** is the expected residential location. The residential location is measured from the full trajectory instead of the trajectory segments. The candidate residential locations are extracted based on records from 00:00 a.m. to 6:00 a.m.

$$\mathbf{RL} = \sum_{j=i_1}^{i_n} \mathbf{r}_j P(j), P(j) \propto t_{j+1} - t_{j-1}$$

- **Activity Radius** r_a is the average distance to a person's residence location:

$$r_a = \frac{1}{i_n - i_1 + 1} \sum_{j=i_1}^{i_n} \text{dis}(\mathbf{r}_{i_j}, \mathbf{RL})$$

where $\text{dis}(x, y)$ is the Euclidean distance.

- **Average Speed** s_{avg} is defined as the average speed of the trajectory segment.
- **Activity Distance** d denotes the length of the trajectory.
- **Time Duration** TD is the time difference between the first and last records of \mathbf{R}_{seg_i} .

For each *move* or *stop* trajectory segment \mathbf{R}_{seg_i} , different features are relevant to characterizing *move* and *stop* segments. Since time duration and distance from residence are important to *stop* segments and path line attributes (entropy, radius of gyration, speed, etc.) are meaningful to *move* segments, we select different feature descriptors to construct the feature vectors \mathbf{F}_i^{move} for *move* and \mathbf{F}_i^{stop} for *stop*.

$$\mathbf{F}_i^{move} = (S^{unc}, S^{tc}, \mathbf{CL}_x, \mathbf{CL}_y, r_g, r_a, s_{avg}, d) \quad (4)$$

$$\mathbf{F}_i^{stop} = (\mathbf{CL}_x, \mathbf{CL}_y, r_a, TD) \quad (5)$$

Consequently, a raw trajectory $\mathbf{R} = \{\mathbf{R}_{seg_1}, \mathbf{R}_{seg_2}, \dots, \mathbf{R}_{seg_n}\}$ is represented by a set of feature vectors:

$$\mathbf{F} = \{\mathbf{F}_1, \mathbf{F}_2, \dots, \mathbf{F}_n\}. \quad (6)$$

2) *Mobility Patterns*: For trajectories of a citywide population, it is inefficient to study human mobility patterns individually. Instead, it is more desirable to group similar trajectory segments from different persons such that the spatiotemporal granularity of mobility can be fairly preserved. In addition, the mobility of a trajectory could be represented with an array of features that is derived with respect to the movement and geographical context.

These considerations require a medium-scale perspective to characterize the mobility behavior. As such, we define a *mobility pattern* as the set of feature vectors (Eq.6) of a group of trajectory segments that are from different persons and share similar mobility behaviors. Thus, a mobility pattern represents the mobility behavior of a group of persons in terms of their contextual geographical, social and lifestyle information.

Given a collection of trajectory segments, a set of mobility patterns can be computed by normalizing the value of feature vectors into the range $[0, 1]$ for each dimension and clustering trajectory segments according to their feature vectors. Since we select different feature descriptors for different trajectory segment types, we employ the standard K-means clustering algorithm to cluster *move* (\mathbf{F}_i^{move}) and *stop* (\mathbf{F}_i^{stop}) separately into K classes where centers are denoted as $\{\mathbf{F}_{C_k}\}, 1 \leq k \leq$

K . We construct K^{move} (K^{stop}) mobility patterns from *move* (*stop*) segments, where $K = K^{move} + K^{stop}$. Then, we denote the feature vectors of each center \mathbf{F}_{C_k} as the mobility pattern of the k th cluster: $\mathbf{MP}_i, 1 \leq i \leq K$.

3) *Parameter Selection*: Picking an appropriate number of clusters remains an open problem, even in the case of traditional k-means. Different values of K reveal human mobility transitions at different granularities. If k is too large, there will be many invalid clusters with fewer members and an increased computational cost. If K is too small, the mobility patterns represented in the clusters will be too general and provide less generalizable insights. Our empirical experiments indicate that the best value of K ranges from 10 to 50. In our case study, we use $K = 20$ ($K^{move} = 10, K^{stop} = 10$).

4) *Mobility Vectors*: To better characterize the transitions among mobility patterns, we compute the proximity of each trajectory segment to each of its K_c nearest cluster centers and represent all proximities with a soft vector quantization technique [17]. The proximity between each trajectory segment and one cluster center is regarded as the similarity of each trajectory segment to the cluster center. Here, K_c is an empirical parameter and is set to be 4 in our experiments. Each trajectory segment is assigned to a mobility vector $\mathbf{m}_i^{move} \in \mathbb{R}^{K^{move}}$ or $\mathbf{m}_i^{stop} \in \mathbb{R}^{K^{stop}}$ with K_c nonzeros according to the segment type by

$$\mathbf{m}_i(j) \propto f(\mathbf{F}_i), f(x) = \exp\left\{-\frac{\|x - \mathbf{F}_{C_j}\|_2}{2w^2}\right\} \quad (7)$$

where $\|x - \mathbf{F}_{C_j}\|_2$ is the Euclidean distance between x and \mathbf{F}_{C_j} , $f(x)$ is a Gaussian weighting function for the purposes of smoothing, and w is the width of the Gaussian kernel.

To give a general representation of the mobility vector mentioned above, we extend \mathbf{m}_i^{move} and \mathbf{m}_i^{stop} to be a K dimensional vector \mathbf{m}_i where the 1st to the K^{move} th elements represent mobility patterns with *move* trajectory segments and $K^{move} + 1$ th to K th(= $K^{move} + K^{stop}$) elements encode mobility patterns with *stop* trajectory segments. Then, a trajectory segment is represented as an array of mobility vectors $\mathbf{m}_i \in \mathbb{R}^K$, of which the j th element indicates the probability of the segment belonging to the mobility pattern \mathbf{MP}_j . A mobility vector \mathbf{m}_i is constructed by concatenating K^{stop} (K^{move}) zeros to \mathbf{m}_i^{move} (\mathbf{m}_i^{stop}):

$$\mathbf{m}_i = \begin{cases} (\mathbf{m}_i^{move}, 0, \dots, 0), & \mathbf{R}_{seg_i} \in \text{move} \\ (0, \dots, 0, \mathbf{m}_i^{stop}), & \mathbf{R}_{seg_i} \in \text{stop} \end{cases} \quad (8)$$

For each trajectory segment \mathbf{R}_{seg_i} , we construct a feature vector \mathbf{F}_i for \mathbf{R}_{seg_i} , and represent each feature vector by a mobility vector \mathbf{m}_i . A raw trajectory is represented by a set of mobility vectors: $\mathbf{M} = \{\mathbf{m}_1, \mathbf{m}_2, \dots, \mathbf{m}_n\}$.

E. Generating the Graph

Our main contribution is the adaptive mobility transition graph (AMTG), a time-varying visual representation for characterizing the temporal evolutions and interleaved transitions of clustered trajectory segments and associated mobility patterns. The AMTG is built upon a collection of trajectory segments and their associated mobility patterns.

The AMTG takes a directed graph representation $\mathbf{G} = (\mathbf{V}, \mathbf{E})$ where \mathbf{V} is a combination of a sequence of time-stamped node sets, $\mathbf{V} = \{V^{t_1}, V^{t_2}, \dots\}$, and $V^{t_i} = \{V_1^{t_i}, V_2^{t_i}, \dots, V_K^{t_i}\}$, and K denotes the number of mobility patterns. Each node $V_j^{t_i}$ denotes a group of trajectory segments at t_i which share a mobility pattern and contains four components: the time stamp t_i , the trajectory segments, the associated persons, and the associated mobility pattern $\text{MP}_j^{t_i}$. A directed edge in \mathbf{E} indicates the transfer processes between pairs of nodes, and the weight of each edge encodes the transition probability. The transitions are only considered between two consecutive node sets V^{t_i} to $V^{t_{i+1}}$. The transition probability denotes the matching ratio of trajectory segments in two nodes in two consecutive frames. The set of transition probabilities between V^{t_i} and $V^{t_{i+1}}$ can be computed by calculating a transition matrix \mathbf{A}^{t_i} . Each element of \mathbf{A}^{t_i} , namely, $a_{p,q}^{t_i}$, represents the transition probability of segments in $V_q^{t_i}$ to those in $V_p^{t_{i+1}}$. An AMTG is then constructed through a time-varying linear dynamic system [23] in which edges (transitions) and associated transition probabilities change temporally. This is basically a timeline-graph representation. Two sequential stages are required: computing the node set \mathbf{V} and the edge set \mathbf{E} .

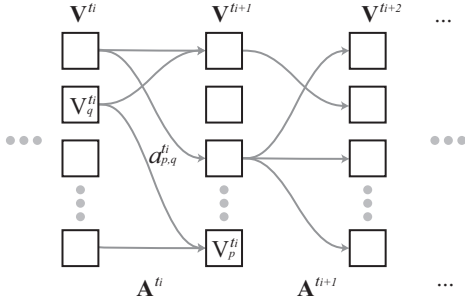


Fig. 2. The conceptual overview of an AMTG.

1) *Computing The Node Set \mathbf{V}* : Suppose that all trajectory segments are categorized into K_m classes of mobility patterns. Because the sequence of trajectory segments of one person are time-varying and nonuniform, two sequences of trajectory segments of two unique persons will not necessarily be aligned along the timeline. Our solution for that is to uniformly re-sample all sequences of trajectory segments along the timeline, e.g., every two hours. This scheme reformulates the sequence set into a time-stamped sequence of mobility patterns, where each frame refers to V^{t_i} . In this way, $V_j^{t_i}$ consists of all trajectory segments whose time durations include t_i and whose feature vectors belong to the mobility pattern MP_j . Its size is: $\text{size}(V_j^{t_i}) = \sum_k I_{V_j^{t_i}}(\mathbf{F}_k)$, where $I_{V_j^{t_i}}(\mathbf{F}_k)$ is an indicator function and \mathbf{F}_k is the feature vector of a trajectory segment. Suppose that the trajectory segment \mathbf{F}_k starts at t_{start} and ends at t_{end} , $I_{V_j^{t_i}}(\mathbf{F}_k) = 1$ if $t_{start} \leq t_i \leq t_{end}$ and \mathbf{F}_k belongs to MP_j , otherwise $I_{V_j^{t_i}}(\mathbf{F}_k) = 0$.

2) *Computing The Edge Set \mathbf{E}* : Directed graphical models, such as Bayesian networks, are a promising tool for analyzing transition patterns [32]. Here, an edge set is the popular transitions recurring across many trajectories. The edge set

has two properties, it is sparse and time-varying [17]. The transition graph is difficult to understand due to a large amount of transitions. It is necessary to filter weak transitions (noisy) and focus on common transitions instead of distal networks. Hence, the edge set should be sparse. The estimation of edge weights may suffer from sparse data (limited transitions occur at a time point t). To overcome the statistical problem of sample scarcity, we utilize the data near t to compute the edge set by re-weighting the transition according to the distance to t . Thus, the weights of the edge set vary smoothly across time and are robust with respect to the time step which we choose to estimate the transition. Bayesian networks are especially suited for learning in such sparse and time-varying structures. Therefore, we adopt a Bayesian networks approach to represent the mobility transitions. \mathbf{E} is computed in two parts:

- The first part is a set of mobility vectors, denoted by $\mathbb{M} = \{\mathbf{M}^1, \dots, \mathbf{M}^L\}$, where L is the count of all persons. Each element $\mathbf{M}^l = \{\mathbf{m}_1^l, \dots, \mathbf{m}_{l_n}^l\}$ is a sequence of mobility vector, and \mathbf{m}_i^l denotes the computed mobility vector described in Section III-D4.
- The second part is a set of time points which denotes the end time of every trajectory segment. It is denoted by $\mathbb{T} = \{\mathbf{T}^1, \dots, \mathbf{T}^L\}$, where L is the person count. Each $\mathbf{T}^l = \{t_1^l, \dots, t_{l_n}^l\}$ denotes a set of sequential time points which are derived from the time stamps of the trajectory segments of the l th person (Eq.2). In other words, $t_1^l, \dots, t_{l_n}^l$ is exactly the end time point of \mathbf{M}^l . Because trajectory segments are not temporally uniform, \mathbf{T}^l is adaptively distributed along the timeline.

The edge set \mathbf{E} represents the transition of mobility patterns. Theoretically, we can estimate the transition matrix $\mathbf{A}^t \in \mathbf{E}$ at arbitrary time points by means of the maximum likelihood method. By assuming that the mobility patterns of each frame are independent from each other, we can model the time-varying mobility dynamics as a time-varying dynamic Bayesian network [32]. We choose to compute \mathbf{E} every 2 hours to achieve a segment-by-segment transition at that time point because all trajectory segments are not temporally aligned. The k -th ($k = 1$) order Gaussian Markovian process is employed:

$$\mathbf{m}_{i+1}^l = \mathbf{A}^{t_i} \mathbf{m}_i^l + \varepsilon, \quad \varepsilon \sim N(0, \sigma^2 I), \quad (9)$$

where ε is a Gaussian noise function, and \mathbf{A}^{t_i} is a $K \times K$ matrix which is time-dependent and changes smoothly and continuously. The dynamic matrix set $\{\mathbf{A}^t, t \in [0, T]\}$ is used to describe the transition graph. For a given t , the transitions between trajectory segments have a varying influence on \mathbf{A}^t , and consequently we re-weight the transitions according to the gap between t_i^l and t (see Fig.2). We assume that the weight follows a Gaussian distribution:

$$w_i^t(i) = \frac{p_h(t - t_i^l)}{\sum_{l=1}^L \sum_{i=1}^{l_n-1} p_h(t - t_i^l)}, \quad p_h(\mu) = \frac{1}{\sqrt{2\pi}h} \exp\left\{-\frac{\mu^2}{2h^2}\right\} \quad (10)$$

where $w_i^t(i)$ is the weight of the transition from \mathbf{m}_i^l to \mathbf{m}_{i+1}^l at t . If t_i^l is close to t , it means that this transition is more reliable for estimating the transition matrix at t . h is the variation of a Gaussian distribution and is used to control the weight of a

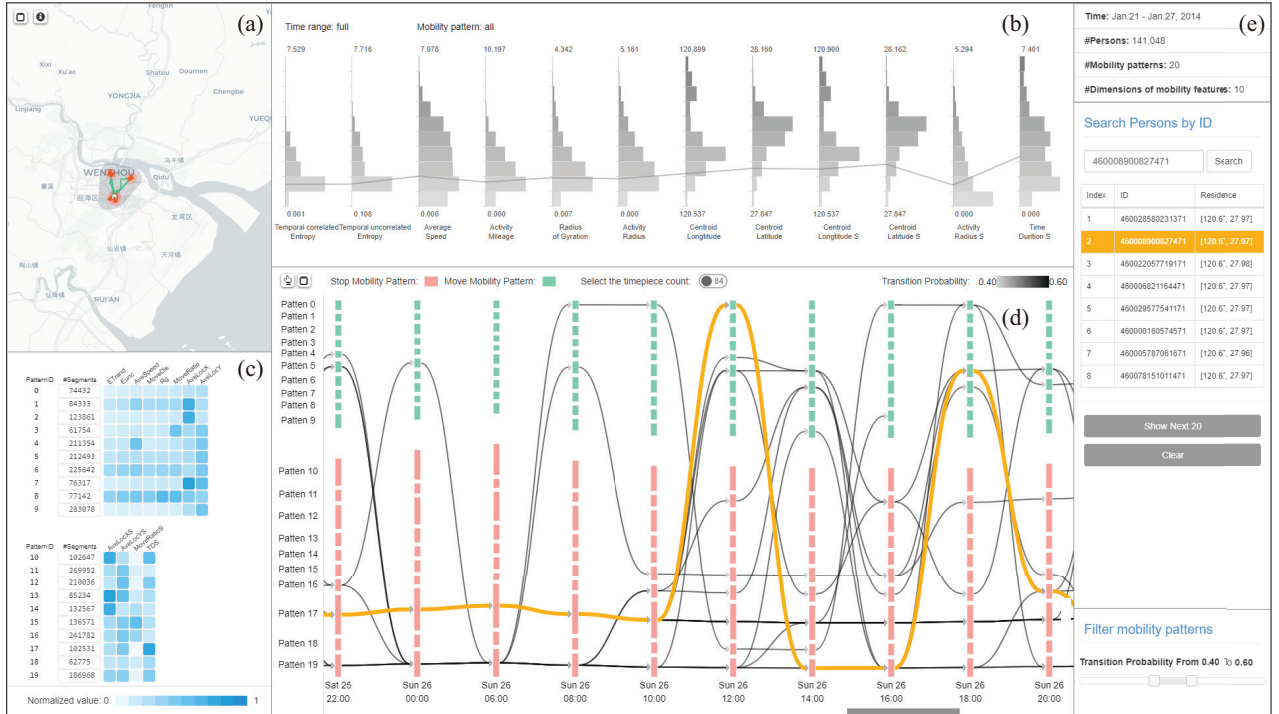


Fig. 3. The mobility patterns extracted from the trajectories of 141,048 persons over 7 days (Jan.21 - Jan.27, 2014). (a) A map view shows the geographical trajectories. (b) The statistical view shows the histogram of each component of the mobility feature. The gray polyline encodes the average mobility features of the selected person. (c) The colored matrix view depicts the feature descriptors of the clustered mobility patterns. (d) An adaptive mobility transition graph is shown with a stacked flow view that illustrates the transitions among time-varying mobility pattern clusters in which each rectangle (a node) encodes a cluster of trajectory segments that exhibit the same mobility pattern at the given time point. The arrow curves in grey between two nodes represent the mobility transition. In this example, the linked curves (in orange) highlight the time-varying mobility of the queried person. (e) The query panel enables users to search for mobility patterns with a given transition probability of specific persons.

trajectory segment. For the sake of efficiency, we estimate \mathbf{A}^t line by line. Finally, we can solve Eq.9 by optimizing a least squares problem with ℓ_1 -norm regularization:

$$\hat{\mathbf{A}}_d^t = \arg \min \left\{ \sum_{l=1}^L \sum_{i=1}^{l_n-1} w_i^t(i) (\mathbf{m}_{i+1,d}^l - \mathbf{A}_d^t \mathbf{m}_i^l) + \lambda \|\mathbf{A}_d^t\|_1 \right\},$$

where d is the d th row of $\hat{\mathbf{A}}_d^t$ and λ is a parameter that controls the sparsity of transition matrix. This not only avoids over-fitting, but also simplifies the resultant graph.

3) *Visualizing The AMTG*: As previously stated, the AMTG is a hybrid timeline-graph representation that characterizes the interconnected mobility transitions in a sequential way. Transition matrices at close time points are very similar because the transition matrix shows the mobility transition over a long time period under the time-varying property described in Section III-E2.

To emphasize the temporal transitions, we calculate the mobility pattern every two hours (e.g., 0:00, 2:00, 4:00,...) since mobility patterns can be very similar in consecutive time points. We estimate a transition matrix at the center of two time points (e.g., 1:00, 3:00, 5:00,...). Since we re-weight the transitions by a Gaussian distribution, we choose the bandwidth parameter h such that the weighting decay is $\exp(1)$ for half of a time step. To show more detail, we also calculate the mobility pattern every hour and estimate transition matrices every hour (e.g., 0:30, 1:30, 2:00,...). We employ an activity-based globally representative time selection [35] method to

filter interested time moments. The importance of a time period is defined as the ratio of the number of mobility pattern transitions to the number of persons.

Our AMTG visualization is similar to Sankey diagrams [29]. We pack the nodes of every \mathbf{V}^{t_i} vertically as a stacked diagram. Each node $V_k^{t_i} \in \mathbf{V}^{t_i}$ represents its corresponding mobility pattern at time point t_i and is visually encoded with a filled rectangle. The height of the rectangle encodes the count of trajectory segments belonging to the mobility pattern. The color of the rectangle encodes the trajectory segment type: red for *stop* segments and green for *move* segments. The nodes can be further classified into two layers according to the trajectory segment type (Fig.3 (d)): a move layer and a stop layer.

The set of \mathbf{V}^{t_i} is sequentially placed from left to right, explicitly representing the transition of mobility patterns over time. The transition between two consecutive $\mathbf{V}_q^{t_i}$ and $\mathbf{V}_p^{t_{i+1}}$ is connected by arrow curves. Its color encodes the transition probability $a_{p,q}^{t_i} \in \mathbf{A}^{t_i}$ from $\mathbf{V}_q^{t_i}$ to $\mathbf{V}_p^{t_{i+1}}$.

IV. VISUAL ANALYSIS

A. The Visual Interface

We design and implement a visual exploration system which consists of a set of linked juxtaposed views. Figure 3 shows an overview of our interface including a map view (Fig.3(a)), a statistics view (Fig.3(b)), a matrix view (Fig.3(c)), an AMTG view (Fig.3(d)) and a query panel (Fig.3(e)).

1) *The Map View*: The map view (Fig.3(a)) shows the geographical information using an OpenStreetMap overlay. The transition of mobility patterns is inherently spatially and temporally correlated. The trajectory of a person or a group of persons is shown as colored curves on the map. The map view applies consistent visual encoding to the nodes in the AMTG view. Each *stop* trajectory segment is encoded with a red circle whose gradient encodes the time duration. Each *move* trajectory is represented as a green curve. To avoid heavy visual clutter, the top-10 trajectory segments whose feature descriptors are the closest to the cluster centroid of a mobility pattern can be shown (Fig.4(a,b)). The trajectory segments of a person can also be displayed (Fig.4(c)). A home glyph is used to show the house location. In addition, we employ a convex hull in grey to provide an overview of the trajectory.

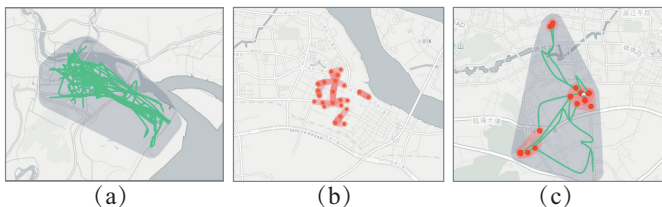


Fig. 4. In the map view, each *move* trajectory segment is encoded as a green curve. A red circle is used to encode a stop trajectory segment. The coverage of the trajectory segments is represented with a convex hull in grey. (a) The top-10 trajectory segments of a node contain a large amount of *move* trajectories. (b) The top-10 trajectory segments of a node contain a large amount of *stop* trajectories. (c) The trajectory of a person.

2) *The Statistics View*: In the statistics view (Fig.3(b)), a vertical bar chart with grey bins encodes the demographic distribution of each component of the feature vector F . The gradient of each bar denotes the value of the corresponding feature. The width of the bars indicate the value ranges of feature descriptors that belong to the pattern. A gray polyline among the binned charts encodes the average mobility features of the selected person.

3) *The Matrix View*: A matrix view (Fig.3(c)) is employed to show the dimensions of each mobility pattern row by row. The color of each cell encodes the average value of each component of its associated feature descriptor. Analysts are able to select a row to study a specific mobility pattern and inspect the corresponding trajectory segments in the map view, the histogram of each component in the statistics view, and the related mobility transition in the AMTG view.

4) *The AMTG View*: The AMTG view (Fig.3(d)) shows an AMTG with the information of each time point. Because the time range of the data is much longer than the view width, analysts can pan the AMTG view to choose time interval for inspection. There are three types of links between nodes:

- The *edges* are represented with curved arrows. Its color encodes the directional transition probability between two time frames. If all edges are shown for an AMTG, heavy visual clutter appears. Analysts can adjust the filtering conditions of the transition probability, e.g., filtering out the probabilities that are out of [0.6, 0.8], yielding a clear visualization of the AMTG that shows edges with strong transition probabilities.

- The correspondence of a specific mobility pattern along the timeline can be represented with a *band* in grey. This is useful to trace the places of a mobility pattern in different time frames.
 - Each trajectory segment is labeled with a mobility pattern (i.e., a node in the AMTG). Thus, the sequence of trajectory segments can be traced as a *path* in grey that links nodes along the timeline (see Fig.3(d)). The *path* of selected person will be highlighted in orange.
- 5) *The Query Panel*: The query panel (Fig.3(e)) supports querying a group of persons by specifying the person id. The trajectory of retrieved persons are shown on other views.

B. Interactive Analysis

The interface offers various possibilities for visually exploring and analyzing the mobility patterns from multiple perspectives. Representative scenarios include:

Explore the mobility transition The analysts can select a node in the AMTG view. The map view and the statistics view show the trajectory and the feature distribution of the selected node. The analysts are able to trace the mobility transition over time by sliding the time bar. Also, when a mobility pattern is chosen in the matrix view, the mobility pattern and the related transitions (edges) will be highlighted.

Explore the mobility of a group of persons A group of persons selected through the querying operations. Our system supports three operations: 1) Querying a person by searching the phone ID encoded in the mobile phone database; 2) Selecting persons whose residences are within the given region created by dragging a rectangle in the map view, and; 3) The analysts can select multiple nodes in the AMTG view. The persons whose paths touch these nodes will be shown. The analysts can select one person and study its mobility pattern.

Explore the feature descriptors The statistics view encodes the demographic distribution of all the feature descriptors by default. When a mobility pattern in the matrix view or a node is selected in the AMTG view, the statistics view represents the distribution of the feature descriptors of the corresponding trajectory segments. When the analysts select one person in the query view, the statistics view shows the average values of all mobility features with a connected polyline among the binned charts (Fig.3(b)).

V. CASE STUDIES

In our study, we chose the trajectory data from Jan. 21, 2014 to Jan. 27, 2014 of 141,048 mobile users, from which 20 mobility patterns are extracted. We conduct two case studies with the help of an expert (a citizen) of the city. We perform trajectory segmentation, feature extraction, and clustering using Java on a PC equipped with a 3.4 GHz Intel Core i7-4770 CPU and 32 GB main memory. Segmentation, feature extraction and clustering take approximately 3 hours. We use a MATLAB toolbox named CVX [13] to estimate the transition matrix in 30 minutes. To support the comprehensive study of mobility behavior, the input of our visualization system includes the raw trajectory data, the adaptive trajectory segments of each person, the constructed mobility patterns, and the constructed AMTG. The total size of data is 38.4 GB.

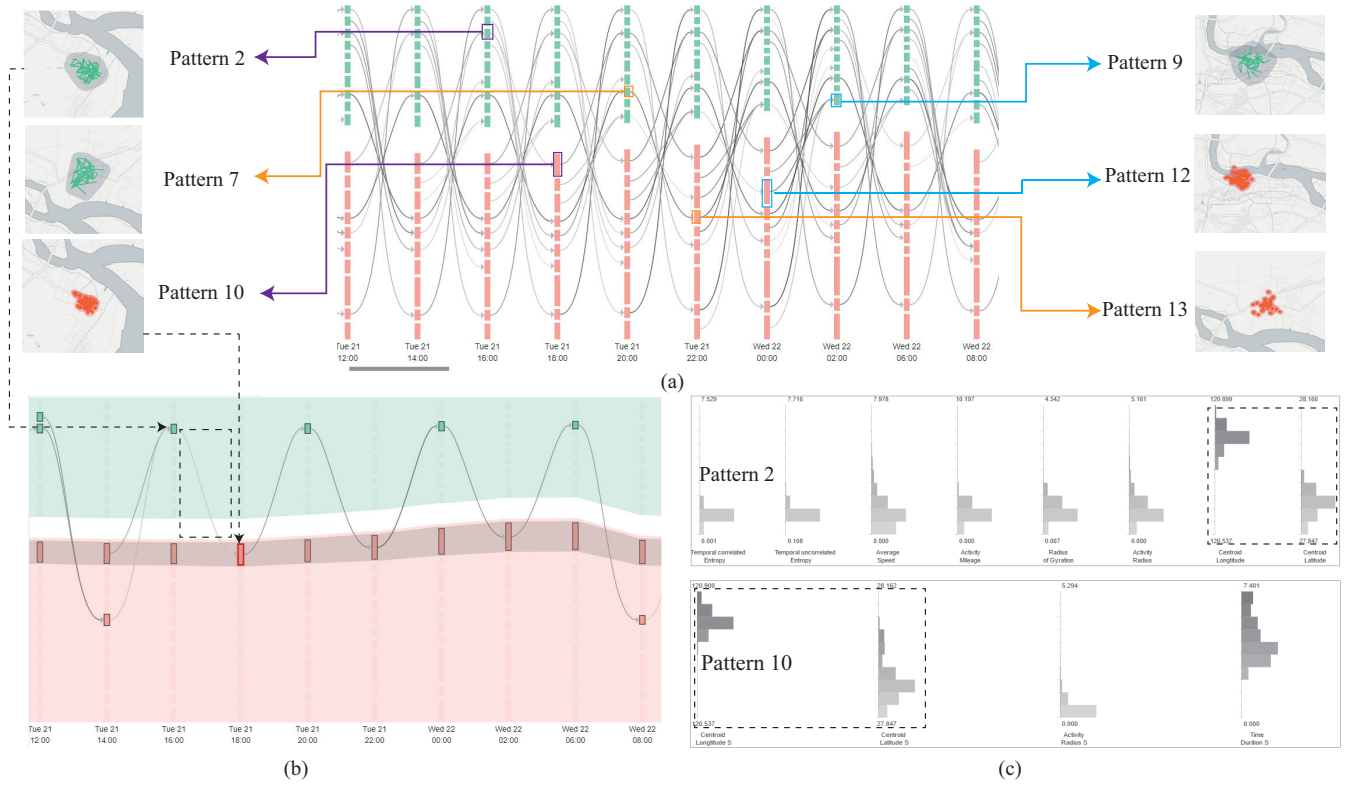


Fig. 5. Studying different mobility patterns with our approach. (a) Three groups of mobility patterns exhibit strong mutual transitions in the AMTG visualization. (b) The transitions between Pattern 2 and Pattern 10. (c) The statistics views of Pattern 2 and Pattern 10.

A. Case 1: Exploring Regions with Different Mobility Patterns

The first case study is designed to explore the mobility patterns and their transitions (Task 1 and Task 2). Based on the AMTG view, we find that the transitions take place among some mobility patterns frequently (Fig.5(a)). By filtering the transition probability to be in $[0.4, 1.0]$, we find three pairs of mobility patterns that exhibit strong mutual transitions: Pattern 9 and Pattern 12, Pattern 2 and Pattern 10, and Pattern 7 and Pattern 13 (Fig.5(a)).

We focus on the pair of Pattern 2 and Pattern 10 for detailed analysis. In the AMTG view (Fig.5(b)), Pattern 10 lies in the stop layer, while Pattern 2 belongs to the move layer. The transition from Pattern 2 to Pattern 10 indicates a sharp transition in terms of moving degree (dotted rectangle in Fig.5(b)). From the map view, we can find that the centroid locations of both patterns are close. This observation is further confirmed by the statistical view (Task 1): the dimensions CL (centroid location) of both patterns are similar (dotted rectangle in Fig.5(c)). In addition, the values of S^{unc} , S^{tc} , s_{avg} , m_a , r_a of Pattern 2 have very low values. A low activity radius and a long time duration of Pattern 10 indicates a lot of people living nearby. The reason for the frequent transitions between Pattern 2 and Pattern 10 is probably that the centroid locations of both patterns are crowded, and their trajectory segments are a mixture of both moving and stationary patterns. By carefully checking the locations, our expert observes that the centroid locations of Pattern 2 and Pattern 10 are in a high-technology developing region, which contains many villages, gardens and office buildings. Persons in the region

may commute between their apartments, offices and gardens.

Analyzing the mobility patterns relies on the geographical and temporal context. For instance, the centroid locations of Pattern 7 and Pattern 13 belong to a small town which is far away from the downtown. Persons in the small town tend to walk after the dinner because there is little traffic. Similarly, the centroid locations of Pattern 9 and Pattern 12 are in a crowded area which has many commercial and cultural facilities. People may come to the area for shopping and meals, yielding frequent transitions between moving and stationary mobilities. In the meantime, the thickness of the stop layer increases progressively with the approaching of night, indicating the willingness to come back to home. This observation is consistent with the fact that people typically leave home for working or studying in the morning.

B. Case 2: Exploring The Mobility Patterns of Island People

To study the living style of the persons on an island of the city, we select a group of persons whose trajectory segments belong to the island at night in 7 days. By studying their trajectory segments on the map view, we find that most of them frequently visit the downtown of the city and stay there for several hours (Fig.6(a)). We additionally select several persons with the help of the query operations provided in the query view (Task 4) and study their traces individually. Fig.6(b) shows that the constructed AMTG and the trace (in orange) of one person. Specifically, the mobility pattern in $[4:00 \text{ am}, 5:00 \text{ am}]$ reveals that the person remains stationary (Task 3). Then the person transits to another mobility pattern in $[5:00$

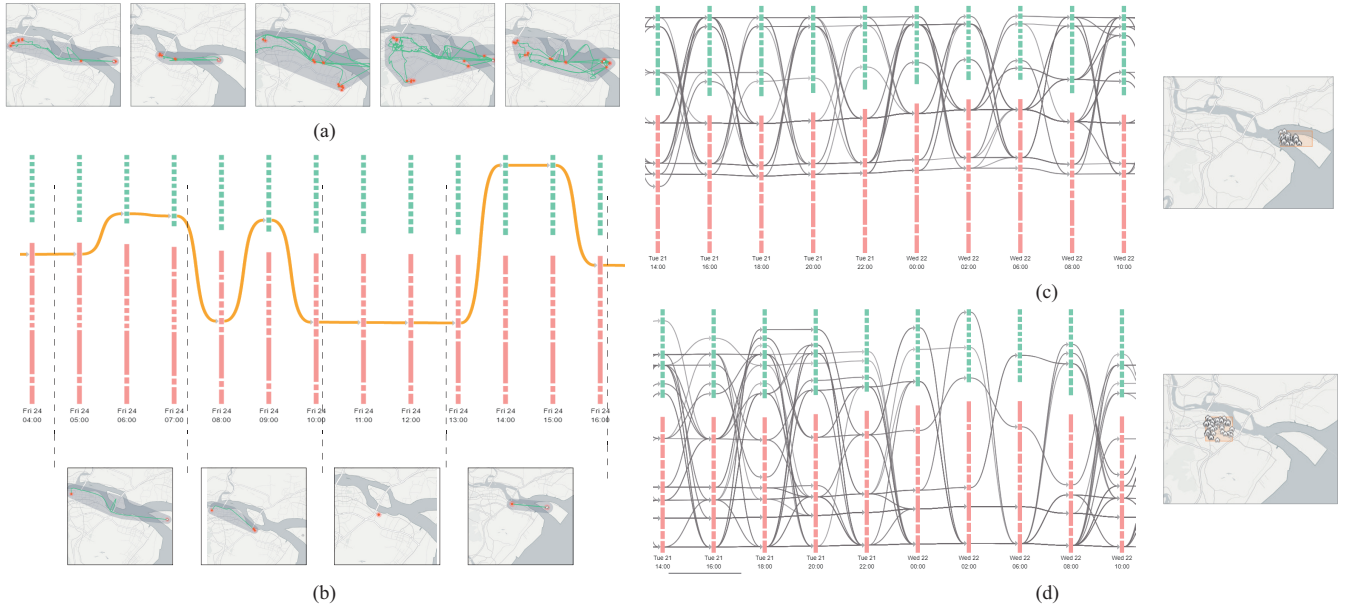


Fig. 6. A group of persons who live on a small island. Most of them visited the downtown center. (a) The trajectories of five persons in one day. (b) The AMTG of one person in one day. (c) The mobility transitions of persons on the island and their corresponding residence locations. (d) The mobility transitions of persons in the downtown and their corresponding residence locations.

am, 6:00 am] (Task 3), which indicates a movement of the person from the island to the downtown (see the trajectory segments on the map). From the AMTG visualization, we can infer that the person stays in a location from 7:00 am to 9:00 am and then traverses to another spot from 9:00 am to 10:00 pm and finally returns to the island at 1:00 pm.

Through the case study, our expert hypothesises that the residents of the island need to go to the downtown for shopping because of the deficiency of the consumption goods. In the meantime, people frequently visit the downtown because they need to purchase goods for the coming Chinese Lunar New Year (4 days after 27th Jan), which is the most significant and long holiday in China.

We further compare the mobility patterns of selected persons on the island and the ones who live in the downtown over 7 days (Task 3 and Task 4). Two groups of persons are identified by querying their residence locations in the map view (Fig.6(c-d)). The traces of the island people along the timeline transition mainly among four mobility patterns, which exhibit three movement behaviors: staying in the island, moving between the island and the downtown, and staying in the downtown. In contrast, the traces of the downtown people exhibit varied mobility patterns, and complicated transitions modes over a short time period.

VI. DISCUSSION AND COMPARISON

In order to demonstrate the strengths of our approach, we compare the proposed AMTG to the Dynamic Categorical Data View (DCDV) methodology proposed by van Landesberger et al. [35]. The DCDV was designed to visualize state transitions over time and focuses on showing the transitions between different locations. However, DCDV employs a sampling method and considers only the transition between two time points. For instance, Fig.7(a) shows an irregular

mobility pattern transition of a single person. When we apply sampling methods to visualize such data, we find this person always belongs to pattern 1 from 10:00 to 12:00 pm. We will lose some information about the activity of pattern 12. To solve this issue, our scheme is designed to modeling all the mobility transitions. We perform an experiment to compare other sampling methods to our scheme. We select a number of persons who have more than one transitions from 10:00 am to 12:00 pm. Fig.7(a) shows the number of transition happening between the two time points in a matrix view. We find that the diagonal of the matrix has a larger value than others. Fig.7(b) shows that the transition happens between mobility patterns with *move* trajectory segments (0-9) and mobility patterns with *stop* trajectory segments (10-19). As such, our proposed scheme can provide higher resolution when modeling all transitions happening within the time period.

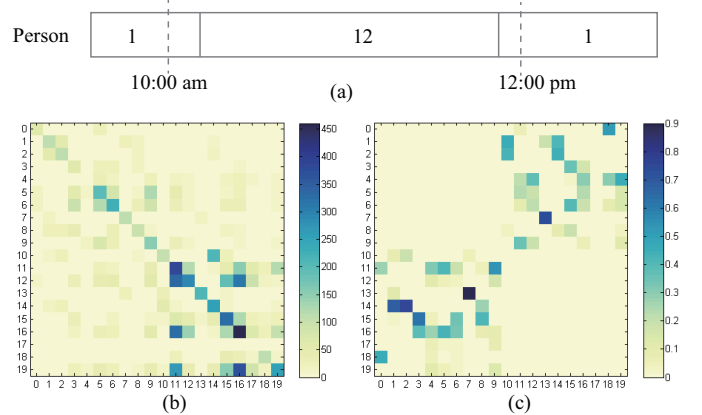


Fig. 7. Comparison of sampling method and our scheme. (a) An irregular mobility pattern transition of a person. (b) The number of transition under sampling method. (c) The transition matrix estimated by our scheme.

Furthermore, previous work has focused primarily on using a uniform temporal segmentation of the data. However, such a segmentation can miss shifts in patterns and create arbitrary cut-offs. For example, commuters may go to work primarily from 8:00 am to 9:00 am, but others may commute from 9:30 am to 10:30 am. Uniform cuts would not group these mobility patterns as having the same behavior. By developing an adaptive methodology the proposed AMTG can help overcome such issues. In Fig.8(b), a person leaves A at 9:30 am, arrives at B at 11:10 am through C, leaves B at 12:50 pm, and arrives A at 2:30 pm. If we divide the trajectory into equal segments: [10:00 am - 12:00 am] and [12:00 am - 2:00 pm], these two trajectory segments share the same feature vector and belong to same mobility pattern (Fig.8(c)) resulting in data loss due to the arbitrary cutoff. However, when we divide the trajectory into stops and moves using the adaptive scheme, we are able to identify traffic behaviors between two places from the AMTG view. As such, the adaptive scheme is more precise in describing the dynamic mobility pattern than a uniform scheme and is one of the principle contributions of this work.

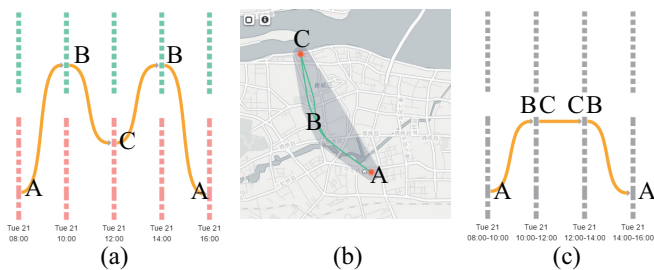


Fig. 8. Comparison of the uniform scheme and the adaptive scheme. A and C are *stop* trajectory segments at two places. B indicates the path connecting A and C. (a) The adaptive scheme (b) Trajectory on the map view (c) The uniform scheme.

VII. FUTURE WORK

The proposed approach has several limitations. First, we find it difficult to place more than 50 nodes due to the limited screen size. Extending the AMTG view to support more than 50 mobility patterns is also an open area for future work. An online hierarchical clustering method can be employed to support interactive exploration of mobility pattern. Second, the constant time threshold is unsuitable for the whole domain. We plan to propose a flexible scheme which takes location and sampling frequency into consideration. Third, although we slice trajectories into stop and move segments by identifying stop records, we do not completely link semantic information into our scheme. As future work, we plan to enrich stop trajectory segments with semantic information, such as points-of-interest data and microblog data, and each move may be annotated with a transportation label, such as bus, walk, bicycle, etc. The mobility pattern can be generated by activities instead of trajectory feature. Such semantic trajectory segments could facilitate a deeper perspective of trajectory data. In this sense, the trajectory of a person over the course of a single day consists of a set of behaviors (e.g., stay at home).

With semantic information, single-day trajectories can be transformed into a list of temporally non-uniform segments, i.e., $(stop, home, \sim 8am) \rightarrow (move, car, 8am \sim 9am) \rightarrow (stop, office, 10am \sim 5pm) \rightarrow (move, car, 5pm \sim 6pm) \rightarrow (stop, home, 6pm \sim)$.

ACKNOWLEDGMENT

This work is supported by the the National 973 Program of China (2015CB352503) and National Natural Science Foundation of China (61772456, U1609217, 61572146, U1501252, U1711263).

REFERENCES

- [1] S. Al-Dohuki, Y. Wu, F. Kamw, J. Yang, X. Li, Y. Zhao, X. Ye, W. Chen, C. Ma, and F. Wang. SemanticTraj: A New Approach to Interacting with Massive Taxi Trajectories. *IEEE Transactions on Visualization and Computer Graphics*, 23(1):11–20, Jan 2017.
- [2] G. Andrienko, N. Andrienko, S. Rinzivillo, M. Nanni, D. Pedreschi, and F. Giannotti. Interactive visual clustering of large collections of trajectories. In *IEEE Symposium on Visual Analytics Science and Technology*, pages 3–10, Oct 2009.
- [3] M. Ankerst, M. M. Breunig, H.-P. Kriegel, and J. Sander. Optics: Ordering points to identify the clustering structure. In *ACM SIGMOD International Conference on Management of Data, SIGMOD '99*, pages 49–60, New York, NY, USA, 1999. ACM.
- [4] A.-L. Barabasi. The origin of bursts and heavy tails in human dynamics. *Nature*, 435(7039):207–211, 2005.
- [5] D. R. Basgeet, P. Dugenie, A. Munro, D. Kalessi, and J. Irvine. SMM: Mathematical framework of a scalable mobility model. In *ACM International Workshop on Modeling Analysis and Simulation of Wireless and Mobile Systems*, pages 74–81, 2003.
- [6] C. Bettstetter. Mobility modeling in wireless networks: Categorization, smooth movement, and border effects. *ACM SIGMOBILE Mobile Computing and Communications Review*, 5(3):55–66, 2001.
- [7] J.-Y. L. Boudec and M. Vojnovic. Perfect simulation and stationarity of a class of mobility models. In *IEEE Conference on Computer and Communications Societies*, volume 4, pages 2743–2754, 2005.
- [8] E. Cho, S. A. Myers, and J. Leskovec. Friendship and mobility: User movement in location-based social networks. In *ACM SIGKDD*, pages 1082–1090, 2011.
- [9] D. Chu, D. A. Sheets, Y. Zhao, Y. Wu, J. Yang, M. Zheng, and G. Chen. Visualizing hidden themes of taxi movement with semantic transformation. In *IEEE PacificVis*, pages 137–144, 2014.
- [10] Y.-A. de Montjoye, C. A. Hidalgo, M. Verleysen, and V. D. Blondel. Unique in the Crowd: The privacy bounds of human mobility. *Scientific reports*, 3, 2013.
- [11] M. Gonzalez. Unraveling daily human mobility motifs. In *2013 IEEE/ACM International Conference on Advances in Social Networks Analysis and Mining (ASONAM 2013)*, pages xxxviii–xxxviii, Aug 2013.
- [12] M. C. Gonzalez, C. A. Hidalgo, and A.-L. Barabasi. Understanding individual human mobility patterns. *Nature*, 453(7196):779–782, 2008.
- [13] M. Grant and S. Boyd. CVX: Matlab software for disciplined programming, version 1.2, 2015.
- [14] S. Gupta, M. Dumas, M. J. McGuffin, and T. Kapler. Movementslicer: Better gantt charts for visualizing behaviors and meetings in movement data. In *IEEE PacificVis*, pages 168–175, 2016.
- [15] S. Havre, B. Hetzler, and L. Nowell. ThemeRiver: Visualizing theme changes over time. In *IEEE Symposium on Information Visualization*, pages 115–123, 2000.
- [16] C. Joumaa. *Spatiotemporal Characterization of Scalable Data Analysis and Mobility Stochastic Modeling. Application for Urban Planning and Transport Infrastructure*. Theses, Université de Technologie de Belfort-Montbéliard, Nov. 2010.
- [17] G. Kim and E. P. Xing. Reconstructing storyline graphs for image recommendation from web community photos. In *IEEE Conference on Computer Vision and Pattern Recognition*, 2014.
- [18] S. Kisilevich, F. Mansmann, M. Nanni, and S. Rinzivillo. *Spatiotemporal clustering*, pages 855–874. Springer US, Boston, MA, 2010.
- [19] J.-G. Lee, J. Han, and K.-Y. Whang. Trajectory Clustering: A Partition-and-group Framework. In *ACM SIGMOD*, pages 593–604. ACM, 2007.

- [20] D. Liu, D. Weng, Y. Li, J. Bao, Y. Zheng, H. Qu, and Y. Wu. SmartADP: Visual Analytics of Large-scale Taxi Trajectories for Selecting Billboard Locations. *IEEE Transactions on Visualization and Computer Graphics*, 23(1):1–10, Jan 2017.
- [21] S. Liu, D. Maljovec, B. Wang, P. T. Bremer, and V. Pascucci. Visualizing high-dimensional data: Advances in the past decade. *IEEE Transactions on Visualization and Computer Graphics*, 23(3):1249–1268, 2017.
- [22] X. Lu, L. Bengtsson, and P. Holme. Predictability of population displacement after the 2010 Haiti earthquake. *Proceedings of the National Academy of Sciences*, 109(29):11576–11581, 2012.
- [23] J. Luttinen, T. Raiko, and A. Ilin. Linear state-space model with time-varying dynamics. In *Machine Learning and Knowledge Discovery in Databases*, pages 338–353. Springer, 2014.
- [24] N. Mamouli. *Encyclopedia of database systems*, chapter Spatio-Temporal Data Mining, pages 2725–2730. Springer, 2009.
- [25] F. Miranda, H. Doraiswamy, M. Lage, K. Zhao, B. Gonçalves, L. Wilson, M. Hsieh, and C. T. Silva. Urban Pulse: Capturing the Rhythm of Cities. *IEEE Transactions on Visualization and Computer Graphics*, 23(1):791–800, Jan 2017.
- [26] N. Navet and S.-H. Chen. On predictability and profitability: Would gp induced trading rules be sensitive to the observed entropy of time series? In *Natural Computing in Computational Finance*, pages 197–210. Springer, 2008.
- [27] W. Navidi and T. Camp. Stationary distributions for the random waypoint mobility model. *IEEE Transactions on Mobile Computing*, 3(1):99–108, 2004.
- [28] N. Pelekis, I. Kopanakis, G. Marketos, I. Ntoutsis, G. Andrienko, and Y. Theodoridis. Similarity Search in Trajectory Databases. In *Temporal Representation and Reasoning*, pages 129–140, June 2007.
- [29] P. Riehmman, M. Hanfler, and B. Froehlich. Interactive sankey diagrams. In *IEEE Symposium on Information Visualization*, pages 233–240, 2005.
- [30] S. Rinzivillo, D. Pedreschi, M. Nanni, F. Giannotti, N. Andrienko, and G. Andrienko. Visually driven analysis of movement data by progressive clustering. *Information Visualization*, 7(3):225–239, June 2008.
- [31] C. Song, Z. Qu, N. Blumm, and A.-L. Barabási. Limits of predictability in human mobility. *Science*, 327(5968):1018–1021, 2010.
- [32] L. Song, M. Kolar, and E. P. Xing. Time-varying dynamic bayesian networks. In Y. Bengio, D. Schuurmans, J. D. Lafferty, C. K. I. Williams, and A. Culotta, editors, *Advances in Neural Information Processing Systems*, pages 1732–1740. Curran Associates, Inc., 2009.
- [33] S. Spaccapietra, C. Parent, M. L. Damiani, J. A. de Macedo, F. Porto, and C. Vangenot. A conceptual view on trajectories. *Data & Knowledge Engineering*, 65(1):126 – 146, 2008.
- [34] J. Treurniet. A taxonomy and survey of microscopic mobility models from the mobile networking domain. *Acm Computing Surveys*, 47(1):14:1–14:32, 2014.
- [35] T. von Landesberger, S. Bremm, N. Andrienko, G. Andrienko, and M. Tekušová. Visual analytics methods for categoric spatio-temporal data. In *IEEE Conference on Visual Analytics Science and Technology (VAST)*, pages 183–192. IEEE, 2012.
- [36] J. Wang, D. Wei, K. He, H. Gong, and P. Wang. Encapsulating urban traffic rhythms into road networks. *Scientific reports*, 4, 2014.
- [37] K. H. Wang and B. Li. Group mobility and partition prediction in wireless ad-hoc networks. In *IEEE International Conference on Communications*, volume 2, pages 1017–1021, 2002.
- [38] P. Wang, T. Hunter, A. M. Bayen, K. Schechtner, and M. C. González. Understanding road usage patterns in urban areas. *Scientific reports*, 2, 2012.
- [39] Z. Yan, D. Chakraborty, C. Parent, S. Spaccapietra, and K. Aberer. Semantic trajectories: Mobility data computation and annotation. *ACM Transactions on Intelligent Systems and Technology*, 4(3):49:1–49:38, 2013.
- [40] Z. Yan, C. Parent, S. Spaccapietra, and D. Chakraborty. A hybrid model and computing platform for spatio-semantic trajectories. In *The Semantic Web: Research and Applications*, pages 60–75. Springer Berlin Heidelberg, Berlin, Heidelberg, 2010.
- [41] J. J.-C. Ying, W.-C. Lee, T.-C. Weng, and V. S. Tseng. Semantic trajectory mining for location prediction. In *ACM SIGSPATIAL International Conference on Advances in Geographic Information Systems*, pages 34–43, 2011.
- [42] V. W. Zheng, Y. Zheng, X. Xie, and Q. Yang. Collaborative location and activity recommendations with GPS history data. In *International Conference on World Wide Web*, pages 1029–1038, 2010.



Tianlong Gu received the MEng degree from Xidian University, China, in 1987, and the PhD degree from Zhejiang University, China, in 1996. From 1998 to 2002, he was a research fellow in the School of Electrical and Computer Engineering, Curtin University of Technology, Australia, and a post-doctoral fellow in the School of Engineering, Murdoch University, Australia. He is currently a professor in the School of Computer Science and Engineering, Guilin University of Electronic Technology, China.



Minfeng Zhu received his B.S. in mathematics from the Zhejiang University, China in 2015. He is currently a PhD student in the College of Computer Science and Technology at the Zhejiang University. His research interests include visualization and visual analysis of urban data.



Wei Chen is a professor at the State Key Lab of CAD&CG, Zhejiang University. His research interests is on visualization and visual analysis, and has published more than 30 IEEE/ACM Transactions and IEEE VIS papers. He actively served as guest or associate editors of IEEE Transactions on Visualization and Computer Graphics, IEEE Transactions on Intelligent Transportation Systems, and Journal of Visualization. For more information, please refer to <http://www.cad.zju.edu.cn/home/chenwei/>



Zhaosong Huang received his B.S. in computer science from the Shandong University, China in 2015. He is currently a PhD student in the College of Computer Science and Technology at the Zhejiang University of State Key Lab of CAD&CG. His research interests include visualization and visual analysis of urban data.



Ross Maciejewski is an Associate Professor at Arizona State University in the School of Computing, Informatics Decision Systems Engineering. My primary research interests are in the areas of geographical visualization and visual analytics focusing on public health, dietary analysis, social media, criminal incident reports, and the food-energy-water nexus. I have served on the organizing committee for the IEEE Conference on Visual Analytics Science and Technology and the IEEE/VGTC EuroVis Conference. I am a recipient of an NSF CAREER Award (2014) and was recently named a Fulton Faculty Exemplar and Global Security Fellow at Arizona State



Liang Chang is a professor at the Department of Computer and Control, Guilin University of Electronic Technology. His research interests include knowledge representation and reasoning, description logics, intelligent agents, and the Semantic Web. He received his PhD in computer science from the Institute of Computing Technology, Chinese Academy of Sciences.